PCCP

Physical Chemistry Chemical Physics

COVER ARTICLE
Bryce *et al.*
Solid-state $^{185/187}$Re NMR spectral evidence for the origin of high-order quadrupole-induced effects

HOT ARTICLE
Dolnik *et al.*
Locking of Turing patterns in the chlorine dioxide–iodine–malonic acid reaction

Definitive solid-state $^{185/187}$Re NMR spectral evidence for and analysis of the origin of high-order quadrupole-induced effects for $I = 5/2$†

Cory M. Widdifield,[a] Alex D. Bain[b] and David L. Bryce*[a]

Rhenium-185/187 solid-state nuclear magnetic resonance (SSNMR) experiments using NaReO$_4$ and NH$_4$ReO$_4$ powders provide unambiguous evidence for the existence of high-order quadrupole-induced effects (HOQIE) in SSNMR spectra. Fine structure, not predicted by second-order perturbation theory, has been observed in the $^{185/187}$Re SSNMR spectrum of NaReO$_4$ at 11.75 T, where the ratio of the Larmor frequency (ν_0) to the quadrupole frequency (ν_Q) is $\sim$2.6. This is the first experimental observation that under static conditions, HOQIE can directly manifest in SSNMR powder patterns as additional fine structure. Using NMR simulation software which includes the quadrupole interaction (QI) exactly, extremely large $^{185/187}$Re nuclear quadrupole coupling constants (C_Q) are accurately determined. QI parameters are confirmed independently using solid-state $^{185/187}$Re nuclear quadrupole resonance (NQR). We explain the spectral origin of the HOQIE and provide general guidelines that may be used to assess when HOQIE may impact the interpretation of the SSNMR powder pattern of any spin-5/2 nucleus in a large, axially symmetric electric field gradient (EFG). We also quantify the errors incurred when modeling SSNMR spectra for any spin-5/2 nucleus within an axial EFG using second-order perturbation theory. Lastly, we measure rhenium chemical shifts in the solid state for the first time.

Introduction

All quadrupolar nuclei (*i.e.*, $I > 1/2$) possess a nuclear electric quadrupole moment (Q), which will couple with the electric field gradient (EFG) at the nucleus.[1] The coupling between Q and the EFG, known as the quadrupole interaction (QI), provides information that can be used to complement other solid-state nuclear magnetic resonance (SSNMR) observables, such as the isotropic chemical shift (CS). Unfortunately, the QI may also drastically broaden the SSNMR signal in powdered samples, sometimes to the extent that the experiment becomes impractical. Despite this potential drawback, SSNMR experiments using quadrupolar nuclei are valuable, as these nuclei can be found in many important areas of chemical research, including biochemistry (*e.g.*, ^{14}N, ^{17}O, ^{23}Na, ^{25}Mg, ^{43}Ca, ^{67}Zn), and materials science (*e.g.*, $^{6/7}$Li, ^{11}B, ^{17}O, ^{27}Al).[2] The precise determination of the QI is therefore of critical importance to correctly characterize a wide variety of systems using SSNMR spectroscopy. Until now, it was most common to use second-order perturbation theory to model SSNMR line shapes (to see how first- and second-order perturbation theory modifies the Zeeman eigenstates, see the ESI, Fig. S1a†); however, as the sensitivity of SSNMR experiments continues to increase, experiments using previously "inaccessible" nuclei are becoming more common and additional care needs to be taken when analyzing the SSNMR spectra of quadrupolar nuclei that experience a very large QI.

Rhenium, a group 7 transition metal, was first detected in 1925, occurs naturally within molybdenum sulfide ores in the earth's crust ($\sim$10^{-7}% abundance), and may exist in at least nine oxidation states (ranging from -1 to $+7$).[3,4] Compounds containing rhenium in a relatively reduced oxidation state, such as Re(III), exhibit metal–metal bonding interactions: for example, K$_2$Re$_2$Cl$_8$ is recognized as containing the first example of a metal–metal quadruple bond.[5] Rhenium metal possesses very high thermal stability, and is present within the high-temperature alloys used to make jet engine parts.[4] In addition, rhenium-containing compounds have been used as catalysts in many types of organic reactions.[6–8] The nuclei of the two

[a] *Department of Chemistry and Centre for Catalysis Research and Innovation, University of Ottawa, 10 Marie Curie Pvt., Ottawa, Ontario, Canada. E-mail: dbryce@uottawa.ca;*
  Fax: +1 613 562 5170; Tel: +1 613 562 5800 ext. 2018
[b] *Department of Chemistry and Chemical Biology, McMaster University, 1280 Main St. W., Hamilton, Ontario, Canada. E-mail: bain@mcmaster.ca for software enquiries*
† Electronic supplementary information (ESI) available: Additional experimental; detailed $^{185/187}$Re NQR/SSNMR experimental acquisition parameters; energy level diagrams for $I = 5/2$ under various relative Zeeman/QI strengths; experimental $^{185/187}$Re NQR spectra of NaReO$_4$ and NH$_4$ReO$_4$; experimental $^{185/187}$Re EFG/CS parameters obtained *via* second-order perturbation theory; V_{33}/B_0 angle corresponding to the low-frequency CT discontinuity using exact QI theory; table of values used to construct Fig. 5. See DOI: 10.1039/c1cp20572b

stable isotopes of rhenium (^{185}Re/^{187}Re) are NMR-active, are present in high natural abundance (37.398(16)% and 62.602(16)% for ^{185}Re and ^{187}Re, respectively),[9] and are quadrupolar ($I(^{185/187}$Re) = 5/2). In addition, they possess relatively high magnetogyric ratios ($\gamma(^{185}$Re) = 6.1057 × 10^7 rad s^{-1} T^{-1}; $\gamma(^{187}$Re) = 6.1682 × 10^7 rad s^{-1} T^{-1}).[10] Despite the potential wealth of diagnostic information that could be extracted using $^{185/187}$Re SSNMR experiments, very few literature reports exist, and they are nearly exclusively restricted to compounds that exhibit very high symmetry,[11–13] or are from experiments carried out at liquid helium temperatures.[14–16] The paucity of $^{185/187}$Re SSNMR studies may be attributed to the very large Q for both NMR-active nuclides ($Q(^{185}$Re) = 2180(20) mb; $Q(^{187}$Re) = 2070(20) mb).[17] In fact, the line-width factor for ^{185}Re is the highest of the stable elements (1.5 × 10^4 relative to ^{1}H).[10] As such, a very small EFG can result in a rhenium QI that broadens the SSNMR powder pattern to the point that it is undetectable. A partial remedy to this problem is to perform the SSNMR experiments within as high an applied magnetic field (B_0) as possible.

As very high magnetic fields (i.e., $B_0 > 18.8$ T) are becoming increasingly available, SSNMR experiments on previously inaccessible nuclei are now potentially feasible, but remain technically challenging as they often require sensitivity-enhancing pulse sequences[18,19] and/or variable offset cumulative spectrum (VOCS) data acquisition.[20–22] Recently, we have shown that subtle "high-order" (i.e., greater than second-order) quadrupole-induced effects (HOQIE) are present in the SSNMR spectra for ^{127}I ($I = 5/2$) at $B_0 = 11.75$ T and 21.1 T for some alkaline earth iodides.[23] In those cases, the observed HOQIE manifested as a non-uniform frequency-dependent shift of the ^{127}I SSNMR spectrum. While high-order perturbation theory may have been useful for modeling these ^{127}I SSNMR line shapes, we used a simulation code that included Zeeman and QI effects exactly,[24,25] as well as ^{127}I NQR experiments, to precisely measure the EFG tensor magnitude, as well as the isotropic iodine chemical shift.

As part of an effort to more generally and completely understand the origin and ramifications of HOQIE on SSNMR spectra for $I = 5/2$ nuclides, we report here $^{185/187}$Re SSNMR spectra for NH$_4$ReO$_4$ and NaReO$_4$ in standard and ultrahigh B_0. Prior $^{185/187}$Re SSNMR measurements on these two compounds highlighted some of the largest QIs ever measured using NMR, although quantitative EFG tensor information could not be extracted for NaReO$_4$.[22] While repeating the prior $^{185/187}$Re SSNMR measurements on NaReO$_4$ at 11.75 T, we observed previously undetected fine structure. Using both second-order perturbation theory and exact QI simulations, we comment upon the origin of the fine structure and also outline some guidelines that are generally applicable when modeling the SSNMR spectra for any $I = 5/2$ nucleus which experiences a large, axially symmetric QI.

Experimental

1 Sample preparation

Both NaReO$_4$ (99.99%) and NH$_4$ReO$_4$ (99.999%) were purchased from Sigma-Aldrich and were received as powders.

Sample purity was confirmed by the manufacturer (ESI, Additional Experimental†). Both compounds are stable under normal conditions. All samples were tightly packed into 4 mm o.d. Bruker magic angle spinning (MAS) ZrO$_2$ rotors.

2 Solid-state $^{185/187}$Re NMR

Experimental data were acquired at the National Ultrahigh-field NMR Facility for Solids in Ottawa and at the University of Ottawa. The Ultrahigh-field Facility experiments used a standard bore Bruker AVANCE II spectrometer, which operates at $B_0 = 21.1$ T ($\nu_0(^1$H) ≈ 900.08 MHz, $\nu_0(^{185}$Re) = 202.738 MHz, and $\nu_0(^{187}$Re) = 204.781 MHz), and a 4 mm Bruker HX MAS probe. The experiments performed at the University of Ottawa used a wide bore Bruker AVANCE spectrometer, which operates at $B_0 = 11.75$ T ($\nu_0(^1$H) ≈ 500.13 MHz, $\nu_0(^{185}$Re) = 112.652 MHz, and $\nu_0(^{187}$Re) = 113.787 MHz), and a 4 mm Bruker HXY MAS probe. The $^{185/187}$Re SSNMR signals were referenced to a 0.1 mol dm^{-3} solution of NaReO$_4$ in D$_2$O at 0.0 ppm. The $^{185/187}$Re pulse lengths used for experiments on NH$_4$ReO$_4$ were established using the solution reference, and include a scaling of the optimized solution pulse by $1/[I + 1/2] = 1/3$ to selectively excite the central transition ($m_I = 1/2 \leftrightarrow -1/2$; CT) of the solid. Due to the excessive width of the $^{185/187}$Re SSNMR signals of NaReO$_4$ (vide infra), the high- and low-frequency pulse lengths were calibrated using the high- and low-frequency CT and satellite transition (ST) discontinuities of the actual powder sample. For further details on the frequency-dependence of the pulse lengths used to acquire the $^{185/187}$Re SSNMR signals of NaReO$_4$, see the ESI, Table S1.†

The $^{185/187}$Re SSNMR signals were acquired using either Solomon (i.e., "solid") echo (i.e., $\pi/2 - \tau_1 - \pi/2 - \tau_2 - acq$)[26–28] or Hahn echo (i.e., $\pi/2 - \tau_1 - \pi - \tau_2 - acq$)[29] pulse sequences (see also the ESI†). Typical parameters were as follows: $\pi/2 = 1.1$ to 1.7 μs; spectral window = 2 MHz; $\tau_1 = 12.75$ to 13.8 μs; recycle delay ≈ 100 ms, and between 512 and 1024 complex time-domain data points were collected per scan. All final SSNMR spectra were prepared using VOCS data acquisition methods.[20–22] This involves stepping the radiofrequency transmitter at uniform offset values, with the acquisition of a 'sub-spectrum' at each step. The offsets used here were 200 and 300 kHz for Hahn and Solomon echo experiments, respectively. For each transmitter setting, between 8192 and 17 500 transients were collected. Each processed sub-spectrum was combined in the frequency domain via co-addition to produce the final spectrum. Due to the temperature dependence of the $^{185/187}$Re QI for these compounds, all experiments were performed at $T = 291.8(0.2)$ K, as monitored via a Bruker 'type-T' thermocouple and regulated using a standard Bruker variable temperature unit. For full experimental details, see the ESI, Table S1.†

3 Solid-State $^{185/187}$Re NQR

All experiments were carried out at the University of Ottawa using the AVANCE spectrometer outlined above. In addition, NQR experiments used a 4 mm Bruker HX MAS probe, and all spectra were acquired using the Hahn echo pulse sequence at $T = 291.8(0.2)$ K. Non-optimized, short (≤ 1.6 μs), high-powered pulses were used as the radiofrequency was varied

until a particular resonance was detected. The offset used while searching for $^{185/187}$Re NQR signals was 200 kHz. For further details, see the ESI, Table S1.†

Results and discussion

1 Rhenium-185/187 solid-state NMR

i Sodium perrhenate, NaReO$_4$. Under ambient conditions, this material crystallizes in the scheelite-type tetragonal structure (space group, $I4_1/a$).[30] The oxygen atoms in the [ReO$_4^-$] cluster arrange themselves in a distorted tetrahedral fashion about the central Re: there are four equivalent Re–O bond distances (r_{ReO} = 1.728 Å); however, the O–Re–O bond angles range from 108.5° to 111.4°.[31] As the structure is not perfectly tetrahedral, the expected EFG at the Re nucleus is nonzero. Indeed, prior $^{185/187}$Re NQR measurements on this system highlight a substantial, axially symmetric (i.e., the asymmetry parameter, $\eta_Q = 0$) and temperature-dependent rhenium QI.[32,33] Previous $^{185/187}$Re NMR measurements are consistent with a large rhenium QI (C_Q(^{185}Re) ∼ 278 MHz and C_Q(^{187}Re) ∼ 268 MHz, where C_Q is the nuclear quadrupole coupling constant), but were not used to precisely determine the rhenium EFG/CS tensor magnitudes.[22] Prior rhenium NQR data collected at T = 296 K found that ν_Q(^{185}Re) = 44.997(0.005) (C_Q(^{185}Re) = 299.98(0.04) MHz) and ν_Q(^{187}Re) = 42.606(0.005) MHz (C_Q(^{187}Re) = 284.04(0.04) MHz) for NaReO$_4$, where ν_Q is the quadrupole frequency (see the footnotes to Table 1 for the definition of ν_Q used here, as well as the ESI, Fig. S1b,† for an energy level diagram for I = 5/2 under NQR conditions).[34] It is clear that there is a large discrepancy between the previously reported NQR and SSNMR results for the rhenium QI of NaReO$_4$. This compound was chosen for study in order to investigate the possible impact of HOQIE in the $^{185/187}$Re SSNMR spectra and to potentially observe rhenium CS effects.

Rhenium-185/187 NQR experiments were performed (ESI, Fig. S2†) and the resulting transition frequencies (Table 1) allow us to confirm that η_Q($^{185/187}$Re) = 0. As the ratio between the $m_I = \pm 3/2 \leftrightarrow \pm 5/2$ and $m_I = \pm 1/2 \leftrightarrow \pm 3/2$ transition frequencies ($|\Delta m_I| = 1$) is exactly 2 within experimental error, we may conclude that there is no evidence of a nuclear electric hexadecapole interaction.[35] Using our new NQR data, we establish that C_Q(^{185}Re) = 300.68(0.02) MHz and C_Q(^{187}Re) = 284.54(0.02) MHz at 291.8 K. The slight

discrepancy between our C_Q($^{185/187}$Re) values and those measured earlier by NQR can be fully attributed to the difference in the respective measurement temperatures.[36]

To measure the rhenium EFG and CS tensors for this sample using SSNMR, we carried out $^{185/187}$Re SSNMR experiments on powdered NaReO$_4$ at B_0 = 11.75 and 21.1 T (Fig. 1 and 2). In the present study, the $^{185/187}$Re SSNMR signals typically overlap one another due to their similar Larmor frequencies. After careful line shape analysis using exact QI simulation software[24] (it is noted here that other exact QI models exist),[37–40] quantitative agreement between the rhenium EFG tensor parameters determined using our $^{185/187}$Re NQR and NMR measurements was established. In addition, we were able to measure for the first time an isotropic rhenium CS in a solid sample (δ_{iso} = 70(40) ppm relative to 0.1 mol dm^{-3} NaReO$_4$ in D$_2$O). This opens up the possibility that $^{185/187}$Re SSNMR experiments could be used to report on the local rhenium bonding environment or the oxidation state (under favorable conditions) in solid samples. Indeed, the sparse solution $^{185/187}$Re NMR literature data highlight a chemical shift range of ∼6800 ppm.[41,42] We were not able to measure rhenium chemical shift anisotropy (CSA) for this sample.

Upon inspection of Fig. 1 and 2, it is immediately clear that the predominantly CT line shapes at both applied fields are very broad (∼16 and 26 MHz for the spectra acquired at B_0 = 21.1 and 11.75 T, respectively), but the most striking aspect of the spectrum at 11.75 T is the presence of unexpected high-intensity discontinuities (i.e., not predicted using second-order perturbation theory; Fig. 1f). It is intriguing that the extra discontinuities do not appear in the $^{185/187}$Re SSNMR spectrum acquired at 21.1 T. This B_0-dependent system response is consistent with the expected behavior of a second-order (or greater) quadrupole-induced effect and can be fully attributed to HOQIE (vide infra). While it is perhaps clear that up to two additional low-frequency discontinuities could be due to the inner ($m_I = 1/2 \leftrightarrow 3/2$) ST (one from each of ^{185}Re and ^{187}Re), second-order perturbation theory still fails rather spectacularly when one applies the correct ^{187}Re EFG tensor parameters (from NQR and exact line shape simulations) and includes the STs within the model (Fig. 1a and d). The high-frequency ^{187}Re CT discontinuity position is over-estimated by ∼1 MHz, as are both the position of the corresponding low-frequency CT discontinuity and that of the $m_I = 1/2 \leftrightarrow 3/2$ ST. Line shape modeling using exact QI

Table 1 Experimental $^{185/187}$Re EFG tensor parameters and isotropic chemical shifts obtained via exact modeling of the quadrupole interaction[a]

Compound	ν_1(^{185}Re)/MHz	ν_2(^{185}Re)/MHz	ν_1(^{187}Re)/MHz	ν_2(^{187}Re)/MHz	$\|C_Q$(^{185}Re)$\|$[b]/MHz	$\|C_Q$(^{187}Re)$\|$/MHz	η_Q	δ_{iso}[c]/ppm
NaReO$_4$	45.102(0.006)	90.204(0.009)	42.681(0.005)	85.362(0.008)	300.68(0.02)	284.54(0.02)	<0.003	70(40)
NH$_4$ReO$_4$	—	35.068(0.010)	—	33.186(0.008)	116.90(0.04)	110.62(0.03)	<0.003	0(40)

[a] Measurement errors are within parentheses and parameter definitions are as follows: $C_Q = eQV_{33}/h$; $\eta_Q = (V_{11}-V_{22})/V_{33}$, where $|V_{11}| \leq |V_{22}| \leq |V_{33}|$; $\delta_{iso} = (\delta_{11} + \delta_{22} + \delta_{33})/3$, where $\delta_{33} \leq \delta_{22} \leq \delta_{11}$. The frequencies ν_1 and ν_2 correspond to the doubly-degenerate single quantum NQR resonance frequencies, which for I = 5/2 and η_Q = 0 can be defined as: $\nu_1 = \nu_Q = 3C_Q/20$ and $\nu_2 = 2\nu_Q = 3C_Q/10$. All measurements were carried out at T = 291.8(0.2) K. SSNMR line shape simulations were performed using exact theory.[24] EFG tensor parameters using NQR data were determined using the procedure outlined by Semin.[54] [b] While C_Q may take any real value, $|C_Q|$ is measured experimentally using NQR/SSNMR. On the basis of our data, we find that the maximum possible value for the ^{185}Re nuclear electric hexadecapole interaction in NaReO$_4$ is ca. 750 Hz.[35] [c] Rhenium chemical shifts are relative to 0.1 mol dm^{-3} NaReO$_4$ in D$_2$O (δ_{iso}($^{185/187}$Re) = 0 ppm).

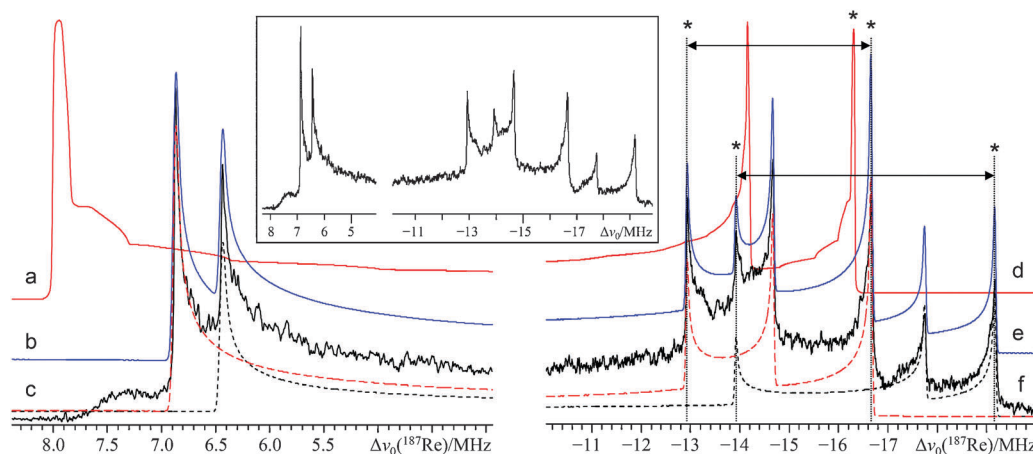**Fig. 1** Second-order perturbation theory simulation (a, d), exact simulation (b, e), and experimental static VOCS Hahn echo (c, f) $^{185/187}$Re SSNMR spectrum of powdered NaReO$_4$, acquired at B_0 = 11.75 T ($\nu_0(^{187}$Re) = 113.787 MHz; $\nu_0(^{185}$Re) = 112.652 MHz) and T = 291.8 K. The second-order perturbation theory spectrum includes only the ^{187}Re signal, to enhance clarity. The high frequency region is depicted in (a, b, c) and the low frequency region is in (d, e, f). Please note that the horizontal scaling is not equivalent between (a, b, c) and (d, e, f): in the inset, the experimental spectrum is displayed using equivalent horizontal scaling for both regions. Below (c and f), the exact simulation line shapes associated with each of ^{185}Re and ^{187}Re are deconvoluted: the long dashed red trace is ^{187}Re, while the short dashed black trace is ^{185}Re. Low-frequency splittings (denoted by double-headed arrows and guide lines) are not predicted by second-order perturbation theory. The discontinuities due to the $m_I = 1/2 \leftrightarrow 3/2$ STs are marked by "*", while the remainder of the discontinuities are due to the $m_I = 1/2 \leftrightarrow -1/2$ transition. All simulations use *identical* EFG tensor parameters, which were also measured independently using $^{185/187}$Re NQR experiments. Minor discontinuities in the slope of trace (a) are due to the POWDER algorithm[55] used for powder averaging.

software leads to both the correct number and frequency positions for all eight observed discontinuities for NaReO$_4$ using the parameters in Table 1. Most importantly, the exact QI model predicts the experimentally observed fine structure in the low-frequency spectral region for both ^{185}Re and ^{187}Re (Fig. 1f). These additional features are field-dependent, are attributed to the $m_I = 1/2 \leftrightarrow 3/2$ ST transition (*vide infra*), and do not interfere with the CT $^{185/187}$Re SSNMR spectra at 21.1 T (Fig. 2).

Although second-order perturbation theory does not predict the correct placement of the CT discontinuities for NaReO$_4$, even at 21.1 T (Fig. 2a), it does predict the correct *number* of discontinuities at the higher applied field. At 21.1 T, the additional fine structure observed at 11.75 T is not present and it appears that HOQIE manifest as a non-uniform frequency-dependent shift in the positions of the discontinuities (with a notable bias towards a positive-frequency shift; the effective parameters determined using second-order perturbation theory are summarized in the ESI, Table S2†). It is therefore clear that the unusual B_0-dependent behavior is due to HOQIE, and that the fine structure observed at 11.75 T must be due to a 3rd-order QI effect on the ST and/or a 4th-order QI effect on the CT and/or ST (as 3rd-order effects on the CT are known to be zero).[43] Beyond 4th-order effects are also potentially significant, but are expected to be much smaller than the leading-order contributions. It is possible that fourth-order perturbation theory may be able to produce accurate line shape models in the regime where the value of ν_Q becomes somewhat comparable to the Larmor frequency (ν_0). Overall, it is seen that second-order perturbation theory cannot lead to the correct values for either δ_{iso} or $C_Q(^{185/187}$Re) under these conditions and in fact both quantities will be underestimated relative to their true values (*vide infra*).

ii Ammonium perrhenate, NH$_4$ReO$_4$. As with NaReO$_4$, NH$_4$ReO$_4$ has the tetragonal scheelite-type structure (space group, $I4_1/a$).[44] Due to the anomalous dependence of its $^{185/187}$Re NQR transition frequencies with respect to temperature and pressure, NH$_4$ReO$_4$ has been featured in numerous rhenium NQR studies[32,45–50] and one rhenium SSNMR[22] account. All prior reports suggest a large and axially symmetric rhenium QI. Relative to NaReO$_4$, the [ReO$_4$]$^-$ cluster in NH$_4$ReO$_4$ is significantly less distorted from tetrahedral: there are four equivalent Re–O bond distances (r_{ReO} = 1.734 Å) and the unique O–Re–O bond angles are 108.8 and 110.8°. Based upon this information, one would expect the rhenium QI in NH$_4$ReO$_4$ to be reduced relative to that of NaReO$_4$ and indeed this is the case. We have chosen this material for study to establish potential HOQIE in the SSNMR spectra for the case of a more modest rhenium QI and to observe chemical shift effects.

To provide a second independent measure of the $^{185/187}$Re EFG tensor parameters in NH$_4$ReO$_4$, rhenium NQR experiments were performed (see ESI, Fig. S3†) and the measured NQR transition frequencies are summarized in Table 1. Using the rhenium NQR data in tandem with the multiple field $^{185/187}$Re SSNMR data (Fig. 3) (SSNMR data analyzed using exact QI line shape modeling), it is observed that $C_Q(^{185}$Re) = 116.90(0.04) MHz, $C_Q(^{187}$Re) = 110.62(0.03) MHz, and $\eta_Q(^{185/187}$Re) = 0 at T = 291.8 K for this sample. After adjusting for the well-known temperature dependence of the rhenium QI in NH$_4$ReO$_4$, these measurements are fully consistent with prior NQR findings. Unlike the $^{185/187}$Re SSNMR spectra of NaReO$_4$ recorded at 11.75 T, there is no evidence of unexpected additional fine structure in the $^{185/187}$Re CT SSNMR spectrum of NH$_4$ReO$_4$. Using exact QI simulation software, we were able to measure the isotropic rhenium chemical shift for this sample as 0(40) ppm. At the lower applied field, the extracted
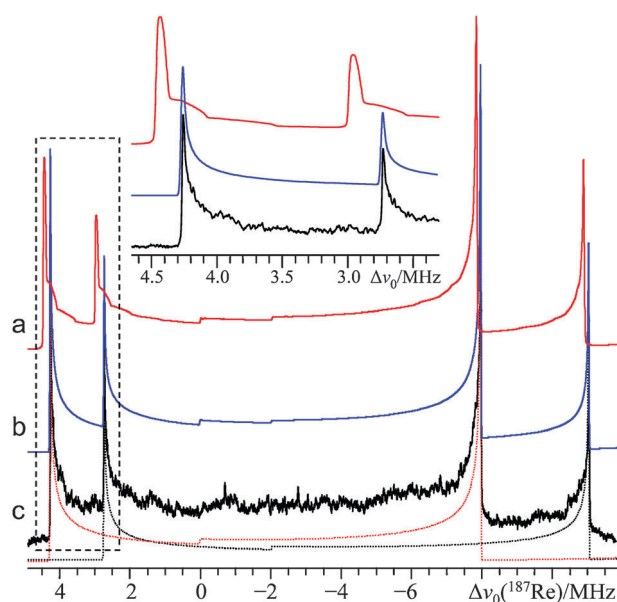
Fig. 2 Second-order perturbation theory simulation (a), exact simulation (b), and experimental static VOCS Solomon echo (c) $^{185/187}$Re SSNMR spectra of powdered NaReO$_4$, acquired at $B_0 = 21.1$ T ($\nu_0(^{187}\text{Re}) = 204.781$ MHz; $\nu_0(^{185}\text{Re}) = 202.738$ MHz) and $T = 291.8$ K. Below c, the exact simulation signals associated with each of ^{185}Re and ^{187}Re are deconvoluted: the dotted red trace is ^{187}Re, while the dotted black trace is ^{185}Re. Low-frequency splittings are not observed; however, the expected positions of the discontinuities in the analytical simulation are subject to a non-uniform, frequency-dependent shift, which is evidence of HOQIE. All simulations used *identical* EFG tensor parameters, which were also measured independently using $^{185/187}$Re NQR experiments. The inset (top, middle) corresponds to the region within the dashed line box, and is meant to highlight the significant difference between the exact and second-order perturbation theory models. For the inset, the deconvolution traces have been omitted to enhance clarity.
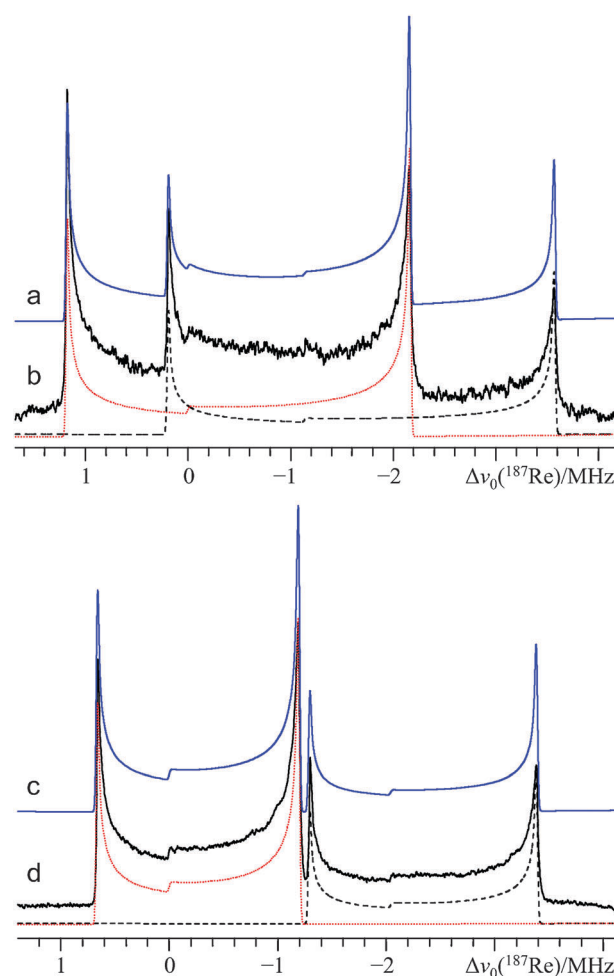

Fig. 3 Exact simulation (a, c), experimental static VOCS Hahn echo (b), and static VOCS Solomon echo (d) $^{185/187}$Re SSNMR spectra of powdered NH$_4$ReO$_4$, acquired at (b) $B_0 = 11.75$ T and (d) $B_0 = 21.1$ T. Below b and d, the exact simulation signals associated with each of ^{187}Re (dotted red trace) and ^{185}Re (dashed black trace) are deconvoluted. All experiments were performed at $T = 291.8$ K.

isotropic chemical shifts using second-order perturbation theory and exact theory do not agree with one another. As was the case in our prior study using ^{127}I SSNMR data,[23] and with the $^{185/187}$Re SSNMR spectral simulations for NaReO$_4$ at 21.1 T, the second-order simulation produces a chemical shift that is smaller than the true value (for the values extracted using second-order perturbation theory, see the ESI, Table S2†). Unlike the rhenium SSNMR line shape simulations for NaReO$_4$, however, the rhenium EFG tensor parameters extracted for NH$_4$ReO$_4$ using both second-order perturbation theory and exact theory match, within experimental error, when modeling the spectrum acquired at 11.75 T. At 21.1 T, quantitative agreement is found between second-order and exact theory for all the reported parameters in Table 1. Hence, there is no evidence of HOQIE in the spectra for NH$_4$ReO$_4$ at 21.1 T and second-order perturbation theory would be sufficient to model this SSNMR line shape. The quantitative agreement for this final case is sensible, as at 21.1 T, the ratio between ν_0 and ν_Q for NH$_4$ReO$_4$ exceeds 10 to 1, which is a regime where HOQIE are not expected to be significant (*i.e.*, the high-field approximation is valid).

As the two CT $^{185/187}$Re signals for NH$_4$ReO$_4$ are separated at 21.1 T (Fig. 3d), and as the central "step" discontinuity is clearly defined for both isotopes, we attempted to include

rhenium CSA in the line shape models for this sample. Unfortunately, the rhenium CS tensor span was too small to be measured and it is noted that the span must be less than *ca.* 80 ppm. A small tensor span is consistent with the nearly tetrahedral local symmetry about the rhenium atoms.

iii Origin of the fine structure present in the $^{185/187}$Re SSNMR spectrum of NaReO$_4$ at 11.75 T. While HOQIE have been observed for several different ν_0/ν_Q ratios in the current study, and while it appears as though the onset of these effects leads to a non-uniform frequency-dependent shift in the resulting SSNMR powder pattern, the $^{185/187}$Re SSNMR spectrum of NaReO$_4$ acquired at 11.75 T presents previously unobserved fine structure. This fine structure was attributed to HOQIE and we now briefly outline its origin and the ν_0/ν_Q regime where it may manifest in an SSNMR spectrum where $I = 5/2$ and $\eta_Q = 0$.

In Fig. 4, line shape simulations are presented which were generated using the exact simulation software. We examined
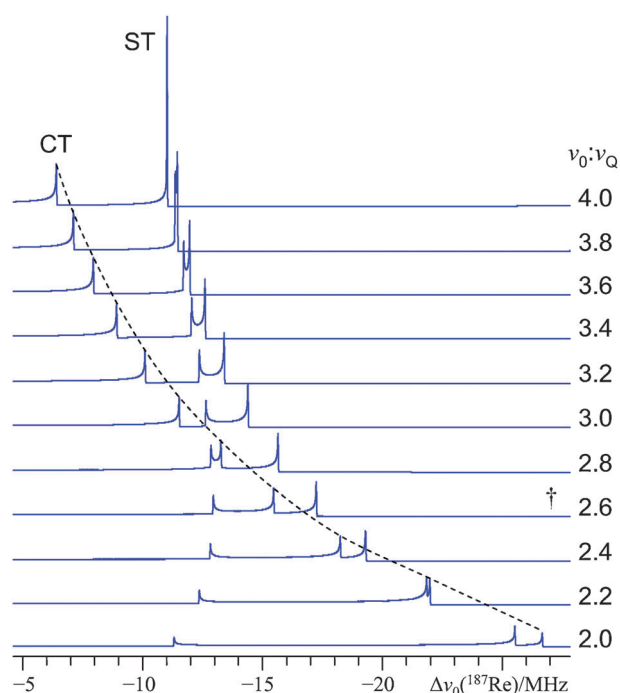
Fig. 4 Exact simulations of the low-frequency spectral region (part of the CT and $m_I = 1/2 \leftrightarrow 3/2$ ST discontinuities only), which highlight the onset and origin of the HOQIE fine structure for NaReO₄. For this particular simulation, the ^{187}Re nucleus at 11.75 T has been assumed; hence, $\nu_0 = 113.787$ MHz. By adjusting ν_Q, the ν_0/ν_Q ratio is varied from 4.0 (top trace) to 2.0 (bottom trace) in steps of −0.2. The dashed line trace clarifies the evolution of the low-frequency CT discontinuity as a function of ν_0/ν_Q. The spectrum corresponding closely to the best-fit spectrum in Fig. 1 is demarked with a dagger above it.

the regime where the ν_0/ν_Q ratio value ranges from 4.0 to 2.0 in steps of −0.2. As we wish to comment upon the origin of the fine structure for this particular case, we have set ν_0 to 113.787 MHz (the value of the NMR resonance condition for the ^{187}Re solution standard at 11.75 T). At $\nu_0/\nu_Q = 4$, it is

noted that the inner ST discontinuity (*i.e.*, $m_I = 1/2 \leftrightarrow 3/2$) is expected to have a relatively high intensity, and there is no additional fine structure. However, as the ν_0/ν_Q value is further decreased, the inner low-frequency ST splits into two discontinuities. Eventually, the discontinuities shift to such an extent that they will both occur within the spectral region which is normally (using second-order perturbation theory) attributed to the CT. For the experimental case of $^{185/187}$Re SSNMR of NaReO₄ at 11.75 T, the ν_0/ν_Q value is roughly 2.6 : 1, which closely resembles the ratio used to generate the trace indicated using a dagger in Fig. 4. Hence, we may conclude that the experimentally observed fine structure is due to a high-order splitting in the $m_I = 1/2 \leftrightarrow 3/2$ ST for each of the ^{185}Re and ^{187}Re nuclides. One can expect this type of fine structure to exist (although it will not likely interfere with the CT signal until $\nu_0/\nu_Q < 3$) once ν_0/ν_Q becomes less than 4. This effect on the ST appears to be similar in nature to the splittings observed in certain STMAS experiments, which were attributed to a third-order quadrupole-induced effect.[51] Fine structure due to third-order effects is also predicted to arise in ^{14}N ($I = 1$) MAS NMR spectra when the value of C_Q becomes large, although it appears that this has not been experimentally validated.[52]

2 General guidelines for NMR spectral analysis when any $I = 5/2$ nucleus experiences a very large, axial QI

It is well known that second-order perturbation theory is a valid method to model many SSNMR line shapes associated with half-integer quadrupolar nuclei; however, care must be taken to ensure that the high-field condition is satisfied (often taken as $\nu_0 > 10\nu_Q$). For a large enough QI (*i.e.*, $\nu_0 < 4\nu_Q$), it was established above, using experiment and theory, that additional fine structure is present in the SSNMR spectrum. Under these conditions, second-order perturbation theory does not even predict the correct number of discontinuities, and it is not meaningful to quantify the differences in the extracted NMR parameters between perturbation theory and
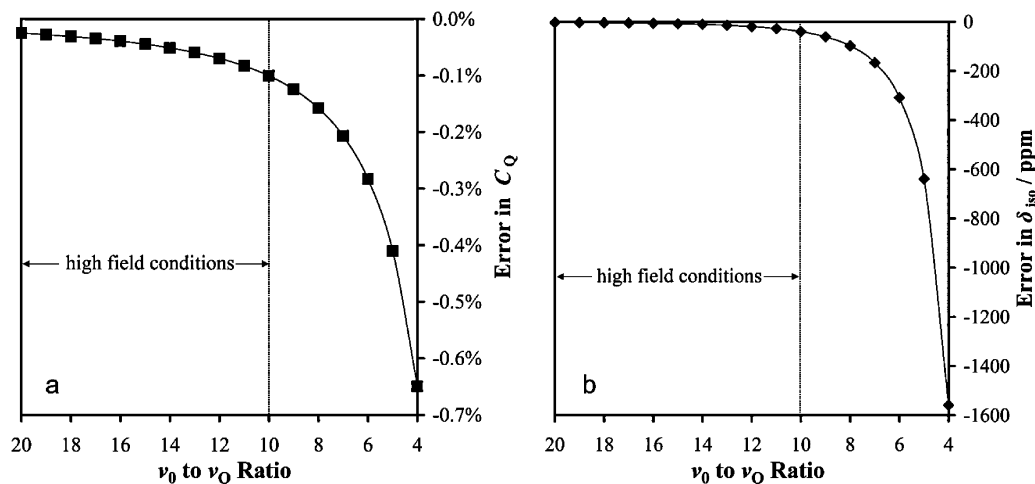

Fig. 5 Illustrations of the errors associated with using second-order perturbation theory to model SSNMR line shapes for the case where $I = 5/2$ and $\eta_Q = 0$, relative to an exact simulation. (a) Error in the C_Q value as a function of the ν_0/ν_Q ratio, and (b) error in the isotropic chemical shift value as a function of the ν_0/ν_Q ratio. High field conditions are traditionally assumed to be satisfied if $\nu_0/\nu_Q > 10$. The lines connecting the data points are guides for the eyes only.

exact theory. Between these two cases, therefore, there exists a region where the high field approximation is not clearly valid, but the additional fine structure is not observable. We comment here upon the errors in the SSNMR parameters extracted (namely C_Q and δ_{iso}) in this intermediate regime when using second-order perturbation theory as compared to exact theory. Methodology details for this section can be found in the ESI, Additional Experimental.†

We consider here the case where a nuclear spin having $I = 5/2$ is subjected to an axial EFG and B_0. The inclusion of additional effects, such as $\eta_Q \neq 0$, CSA, dipole–dipole, etc., is beyond the scope of the current study. For cases where the high-field approximation is traditionally viewed as being valid ($\nu_0 > 10\nu_Q$), it is found that the error in the extracted C_Q value is at most ca. 0.1% (Fig. 5a). However, the error in the isotropic chemical shift, even within the high-field condition, can be as large as 40 ppm (Fig. 5b). For a fictitious example where $\nu_0 = 100$ MHz and $\nu_Q = 10.0$ MHz (i.e., $C_Q = 66.7$ MHz), this would mean an error in the C_Q value of ~67 kHz, while the error in the shift would be 4.0 kHz. As the value of the ratio between ν_0 and ν_Q is decreased (i.e., increasing C_Q or decreasing ν_0), a point is reached where the extracted C_Q and δ_{iso} values exceed typical experimental measurement errors. The point at which this would occur is of course highly dependent upon the measurement conditions and the sample. As an additional example, for the case where $\nu_0 = 4\nu_Q$, the error in the chemical shift extracted using second-order perturbation theory exceeds 1500 ppm (Fig. 5b). At the onset of the additional fine structure ($\nu_0 \approx 4\nu_Q$), the error in the C_Q value determined using second-order perturbation theory will be slightly in excess of 0.6% (Fig. 5a). These findings echo the observations noted previously for spin-5/2 nuclei (although not restricted to $\eta_Q = 0$): when using second-order perturbation theory to model the SSNMR line shapes, the error in the chemical shift becomes detectable at a relatively greater ν_0/ν_Q value than the error in C_Q.[23,53] Importantly, it is observed and calculated that the errors in both parameters will always be such that second-order perturbation theory underestimates the true value of the parameter.

Conclusions

We have presented unambiguous evidence of HOQIE in SSNMR spectra and show that they can manifest in unexpected ways (i.e., not always as simple shifts in the frequencies of the spectral discontinuities). The $^{185/187}$Re NMR spectrum of NaReO$_4$ at $B_0 = 11.75$ T displays additional fine structure in the low-frequency region, which is not predicted by second-order perturbation theory, but which is predicted using an exact QI model. The fine structure is not observed experimentally at 21.1 T, and is not predicted to be present at this field using exact QI line shape simulations, which is in accord with the expected behavior of a quadrupole-induced effect on a SSNMR line shape (i.e., higher B_0 leads to smaller QI spectral effects). We confirm our NMR QI parameters, and rule out (within experimental error) hexadecapole interaction effects by performing $^{185/187}$Re NQR experiments for both samples. We use exact QI simulations to establish that the fine structure will potentially become observable when the ν_0/ν_Q value

drops below 4, and that the fine structure originates from the $m_I = 1/2 \leftrightarrow 3/2$ ST, which also happens to overlap with the CT. For ν_0/ν_Q values greater than 4, we find that the true values of δ_{iso} and C_Q will be underestimated when the spectra are modeled using second-order perturbation theory. Knowledge of HOQIE may be of critical importance for the accurate line shape analysis of SSNMR spectra of many quadrupolar nuclei that may experience large QIs, including $^{63/65}$Cu, ^{67}Zn, ^{75}As, $^{79/81}$Br, ^{91}Zr, ^{105}Pd, ^{115}In, ^{127}I, ^{209}Bi, and others.

Acknowledgements

References

1 C. P. Slichter, Principles of Magnetic Resonance, ed. M. Cardona, P. Fulde, K. von Klitzing, H. J. Queisser and H. K. V. Lotsch, Springer-Verlag, New York, 3rd edn, 1990, pp. 485–502.
2 S. E. Ashbrook, Phys. Chem. Chem. Phys., 2009, 11, 6892.
3 F. A. Cotton and G. Wilkinson, in Advanced Inorganic Chemistry: A Comprehensive Text, Wiley, Toronto, 4th edn, 1980, p. 883.
4 A. V. Naumov, Russ. J. Non-Ferrous Metals, 2007, 48, 418.
5 F. A. Cotton, Acc. Chem. Res., 1969, 2, 240.
6 Y. Kuninobu and K. Takai, Chem. Rev., 2011, 111, 1938.
7 R. Hua and J.-L. Jiang, Curr. Org. Synth., 2007, 4, 151.
8 A. T. Herrmann, T. Saito, C. E. Stivala, J. Tom and A. Zakarian, J. Am. Chem. Soc., 2010, 132, 5962.
9 I. L. Barnes, T. L. Chang, P. De Bièvre, J. W. Gramlich, R. J. C. Hageman, N. E. Holden, T. J. Murphy, K. J. R. Rosman and M. Shima, Pure Appl. Chem., 1991, 63, 991.
10 R. K. Harris, E. D. Becker, S. M. Cabral De Menezes, R. Goodfellow and P. Granger, Pure Appl. Chem., 2001, 73, 1795.
11 M. Bernasson, P. Descouts and G. A. Styles, Helv. Phys. Acta, 1970, 43, 393.
12 J. E. Schirber, L. J. Azevedo and A. Narath, Phys. Rev. B, 1979, 20, 4746.
13 D. G. Klobasa and P. K. Burkert, Magn. Reson. Chem., 1987, 25, 154.
14 A. Narath and D. C. Barham, Phys. Rev., 1968, 176, 479.
15 S. Wada and K. Asayama, J. Phys. Soc. Jpn., 1973, 34, 1163.
16 Y. Nishihara, Y. Yamaguchi, S. Waki and T. Kohara, J. Phys. Soc. Jpn., 1983, 52, 2301.
17 P. Pyykkö, Mol. Phys., 2008, 106, 1965.
18 R. Siegel, T. T. Nakashima and R. E. Wasylishen, Concepts Magn. Reson. A, 2005, 26A, 62.
19 R. Siegel, T. T. Nakashima and R. E. Wasylishen, Concepts Magn. Reson. A, 2005, 26A, 47.
20 D. Massiot, I. Farnan, N. Gautier, D. Trumeau, A. Trokiner and J. P. Coutures, Solid State Nucl. Magn. Reson., 1995, 4, 241.
21 A. Medek, V. Frydman and L. Frydman, J. Phys. Chem. A, 1999, 103, 4830.
22 R. W. Schurko, S. Wi and L. Frydman, J. Phys. Chem. A, 2002, 106, 51.
23 C. M. Widdifield and D. L. Bryce, J. Phys. Chem. A, 2010, 114, 10810.
24 A. D. Bain, Mol. Phys., 2003, 101, 3163.

This journal is © the Owner Societies 2011

Phys. Chem. Chem. Phys., 2011, 13, 12413–12420 | 12419

25 A. D. Bain and B. Berno, *Prog. Nucl. Magn. Reson. Spectrosc.*, 2011, DOI: 10.1016/j.pnmrs.2010.12.002.
26 I. Solomon, *Phys. Rev.*, 1958, **110**, 61.
27 I. D. Weisman and L. H. Bennett, *Phys. Rev.*, 1969, **181**, 1341.
28 A. C. Kunwar, G. L. Turner and E. Oldfield, *J. Magn. Reson.*, 1986, **69**, 124.
29 E. L. Hahn, *Phys. Rev.*, 1950, **80**, 580.
30 A. Atzesdorfer and K.-J. Range, *Z. Naturforsch. B: Chem. Sci.*, 1995, **50**, 1417.
31 J. Spitaler, C. Ambrosch-Draxl, E. Nachbaur, F. Belaj, H. Gomm and F. Netzer, *Phys. Rev. B: Condens. Matter*, 2003, **67**, 115127.
32 A. A. Boguslavskii, R. S. Lotfullin, R. V. Magera and V. V. Pechenov, *Fiz. Tverd. Tela*, 1974, **16**, 2453.
33 R. A. Johnson and M. T. Rogers, in *Advances in Nuclear Quadrupole Resonance: Papers Presented at the International Symposium on Nuclear Quadrupole Resonance, Sept. 28--29, 1972, Queen Elizabeth College, University of London, England*, ed. J. A. S. Smith, 1974, 297.
34 M. T. Rogers and K. V. S. R. Rao, *J. Chem. Phys.*, 1973, **58**, 3233.
35 S. L. Segel, *J. Chem. Phys.*, 1978, **69**, 2434.
36 S. Günther, O. Lutz, A. Nolle and P. G. Schrade, *Z. Naturforsch.*, 1978, **33a**, 1018.
37 G. M. Muha, *J. Magn. Reson.*, 1983, **53**, 85.
38 R. B. Creel and D. A. Drabold, *J. Mol. Struct.*, 1983, **111**, 85.
39 R. B. Creel, *J. Magn. Reson.*, 1983, **52**, 515.
40 B. C. Sanctuary, T. K. Halstead and P. A. Osment, *Mol. Phys.*, 1983, **49**, 753.
41 A. Müller, E. Krickemeyer, H. Bögge, M. Penk and D. Rehder, *Chimia*, 1986, **40**, 50.
42 Y. Do, E. D. Simhon and R. H. Holm, *Inorg. Chem.*, 1985, **24**, 4635.
43 A. D. Bain, *J. Magn. Reson.*, 2006, **179**, 308.
44 I. P. Swainson and R. J. C. Brown, *Acta Crystallogr., Sect. B: Struct. Sci.*, 1997, **53**, 76.
45 K. V. S. R. Rao and M. T. Rogers, *J. Magn. Reson.*, 1972, **8**, 392.
46 P. K. Burkert and M. F. Eckel, *Z. Naturforsch.*, 1973, **28b**, 379.
47 R. A. Johnson and M. T. Rogers, *J. Magn. Reson.*, 1974, **15**, 584.
48 R. J. C. Brown, *J. Magn. Reson.*, 1975, **18**, 558.
49 R. J. C. Brown, J. G. Smeltzer and R. D. Heyding, *J. Magn. Reson.*, 1976, **24**, 269.
50 R. J. C. Brown and S. L. Segel, *J. Chem. Phys.*, 1977, **67**, 3163.
51 S. E. Ashbrook and S. Wimperis, *Prog. Nucl. Magn. Reson. Spectrosc.*, 2004, **45**, 53.
52 S. Cavadini, *Prog. Nucl. Magn. Reson. Spectrosc.*, 2010, **56**, 46.
53 C. M. Widdifield, R. P. Chapman and D. L. Bryce, in *Annu. Rep. Nucl. Magn. Reson. Spectrosc*, ed. G. A. Webb, 2009, vol. 66, 195–326.
54 G. K. Semin, *Russ. J. Phys. Chem. A*, 2007, **81**, 38.
55 D. W. Alderman, M. S. Solum and D. M. Grant, *J. Chem. Phys.*, 1986, **84**, 3717.